Numerical Study of the Influence of Fins' Geometry on the Thermal Performances of a Vertical Shell and Tube Latent Heat Thermal Energy Storage

Teddy Chedid[1,2(✉)], Erwin Franquet[2], Jérôme Pouvreau[1], Pierre Garcia[1], and Jean-Pierre Bédécarrats[3]

[1] Univ. Grenoble Alpes, CEA, LITEN, DTCH, 38000 Grenoble, France
teddy.chedid@cea.fr
[2] Polytech'Lab, Université Côte d'Azur, Nice, France
[3] Universite de Pau et des Pays de l'Adour, E2S UPPA, LaTEP, Pau, France

Abstract. This study consists of evaluating the impact of radial-fins' configurations on natural convection in liquid PCM and on the thermal performances of a vertical shell-and-tube latent heat thermal energy storage system. The design parameters tested are the fin number for a given tube length, the fins' length and type. Results demonstrated that the use of serrated radial fins enhances the heat transferred by natural convection. However, circular fins of the same configurations resulted in a lower total melting time. Furthermore, the results were applied to a storage sizing application to find an optimal configuration for a given design parameters.

Keywords: Shell-and-tube heat exchanger · Phase Change Material · Radial fins · Natural convection · Numerical simulation

1 Introduction

Shell-and-tube latent heat thermal energy storage (LHTES) is a concept where a heat transfer fluid (HTF) flows inside the tubes and transfers heat via the tube's wall to be stored by melting a volume of a Phase Change Material (PCM) occupying the shell [1, 2]. The thermal energy stored while the PCM is in the liquid phase, is then released to the HTF when the process is reversed. This technology can be an important solution to respond to the discrepancy between supply and demand of the energy produced by renewable sources [3] and to recover the waste heat otherwise lost in industrial processes [4]. Therefore, it contributes to the needs for a more sustainable and efficient use of energy.

In a LHTES, several physical phenomena are involved. On the PCM side, the phase change occurs generally at an almost constant temperature. Furthermore, natural convection in the liquid phase may significantly enhance the storage's thermal power [5, 6]. However, most PCMs have a low thermal conductivity and therefore, metallic fins

P. Schossig et al. (Eds.): IRES 2022, AHE 16, pp. 93–110, 2023.
https://doi.org/10.2991/978-94-6463-156-2_8

Table 1. Design parameters of serrated and circular fins for a given tube length (54 cm) and fins thickness (2.5 mm).

Fin number	Pitch (mm)	Fin length (mm)
18	30	22,26,30,34
27	20	22,26,30,34
40	13.5	26,30
54	10	22,26,30,34
80	6.75	26,30

are practically added to the external surface of the heat transfer tubes to intensify the heat exchanged between the HTF and the PCM [7]. The impact of fins' addition on heat transfer dynamics in the storage is widely demonstrated experimentally [8, 9] and numerically [10–13]. Generally, longitudinal fins are selected in the applications with a horizontal tube layout [11, 12] and radial fins for vertical tubes layout [8–10, 13]. Yang et al. [10] demonstrated numerically the impact of natural convection enhancements on the melting progress for a vertical smooth (without fins) and finned tube. The study showed that for a given fin volume ratio and fin height, an optimal design group of fin number, thickness and pitch that maximize the heat transfer rate can be deduced. Karami et al. [9] studied experimentally the impact of perforated circular fins on the thermal performance of a vertical shell-and-tube LHTES. The comparison with solid fins and smooth-tube configurations demonstrated that, due to the improvements of natural convection, the use of perforated circular fins reduces the total melting time and increases the fin effectiveness.

These previous studies showed that the geometric shape of radial fins may significantly impacts natural convection in the liquid phase and ergo, the thermal performance of the storage. The objective of this study is to numerically investigate the influence of several design parameters, namely, the fin number, length and type on the thermal performances and on the enhancements due to natural convection in a vertical shell-and-tube LHTES for a given tube length and fin thickness. Then, the results obtained from the comparison of different fins' configurations applied to a storage component sizing for a charge phase are discussed.

2 Numerical Simulation

2.1 Physical Model

As stated above, this study deals with a vertical shell-and-tubes latent heat thermal energy storage unit with radial fins. Two types of radial fins are studied to investigate the effect of fins' geometry on the system's thermal power (Fig. 1 (a) and (b)). Given the axial symmetry in this case, the 3D geometry of the finned tube is simplified by considering only an angular sector of 22.5° and a tube length of 54 cm, which will reduce the computational cost. For each fin type, several calculations are performed to

Table 2. Material properties

Material	$NaNO_3$	Steel
ρ (kg.m^{-3})	1927	7764
β (K^{-1})	3.8 10^{-4}	-
c_p (J.kg^{-1}.K^{-1})		
Solid	1813	542.8
Liquid	1704	-
λ(W.m^{-1}.K^{-1})		
solid	0.72	50.33
liquid	0.515	-
μ (Pa.s)	2.8 10^{-3}	-
Latent heat L (kJ.kg^{-1})	167.5	-
T_{sol} (°C)	303.3	-
T_{liq} (°C)	306.6	-

investigate the effects of fins' number and length on the melting process of the PCM. Table 1 groups the design parameters for each configuration. The cylindrical tube with an internal diameter of 27.17 mm and a thickness of 2.29 mm as well as the fins are made of carbon steel SA334 Grade 6. The PCM selected is Sodium nitrate ($NaNO_3$) which occupies the volume around the tube extended to the external boundary of a diameter of 102 mm. The thermo-physical properties of the PCM and the steel are listed in Table 2 [14].

2.2 Governing Equations

The PCM is considered as a homogenous, Newtonian fluid, flowing in a laminar regime. The heat transfer and phase change problems are therefore modelled using the enthalpy-porosity method [15]. Fluid motion in the liquid phase is assumed by varying PCM's density according to the Boussinesq approximation. Consequently, PCM volume expansion during melting is neglected. The mass, momentum and energy balance equations are the following:

$$\nabla.\mathbf{u} = 0 \tag{1}$$

$$\rho\left(\frac{\mathrm{d}\mathbf{u}}{\mathrm{dt}} + \mathbf{u}.\nabla\mathbf{u}\right) = -\nabla P + \nabla(\mu\nabla\mathbf{u}) - \rho\beta\big(T - T_{ref}\big)\mathbf{g} + \mathrm{A}\mathbf{u} \tag{2}$$

$$\rho c_p\left(\frac{dT}{dt} + \mathbf{u}.\nabla T\right) = \nabla(\lambda\nabla T) - \rho L\left(\frac{df_m}{dt} + \boldsymbol{u}.\nabla f_m\right) \tag{3}$$

where P is the pressure and $\mathbf{u}$ is the velocity vector. ρ, c_p, λ, μ and β are respectively the density, specific heat capacity, thermal conductivity, dynamic viscosity and the thermal expansion coefficient of the PCM.

While solid, the velocity of the PCM is damped by introducing the term A to the momentum equation. It adopts the following expression:

$$A = A_{mush} \frac{(1 - f_m)^2}{f_m^3 + b} \tag{4}$$

With b = 10^{-3}, a very small value added to prevent division by zero. A_{mush} is the mushy zone constant. Its value has to be large enough to stop the flow in the solid phase. In this study, A_{mush}= 10^8 is considered [16, 17]. f_m is the melted fraction of the PCM, it is defined as:

$$f_m = \begin{cases} 0 & if\ T < T_{sol} \\ \frac{T - T_{sol}}{T_{liq} - T_{sol}} & if\ T_{sol} < T < T_{liq} \\ 1 & if\ T > T_{liq} \end{cases} \tag{5}$$

where T_{sol} and T_{liq} are respectively the solidus and liquidus temperatures.

In the metallic parts, formed by the tube wall and the fins, only the energy equation applies:

$$\rho c_p \frac{\partial T}{\partial t} = \lambda \Delta T \tag{6}$$

For each geometric configuration, a charge phase is simulated using two different heat transfer models to quantify the impact of natural convection in melted PCM on the system's thermal power. To do so, in addition to the model described above, calculations using a second model, named "*conduction-only*" are performed. In this model, only the heat transferred by conduction in the liquid PCM is considered. Therefore, the sole equation to solve is the energy equation (Eq. (3)) where **u = 0.**

Initially, both PCM and finned heat transfer tube are at the same temperature of 290 °C. A fixed and uniform temperature of 315 °C is imposed on the inner tube wall.

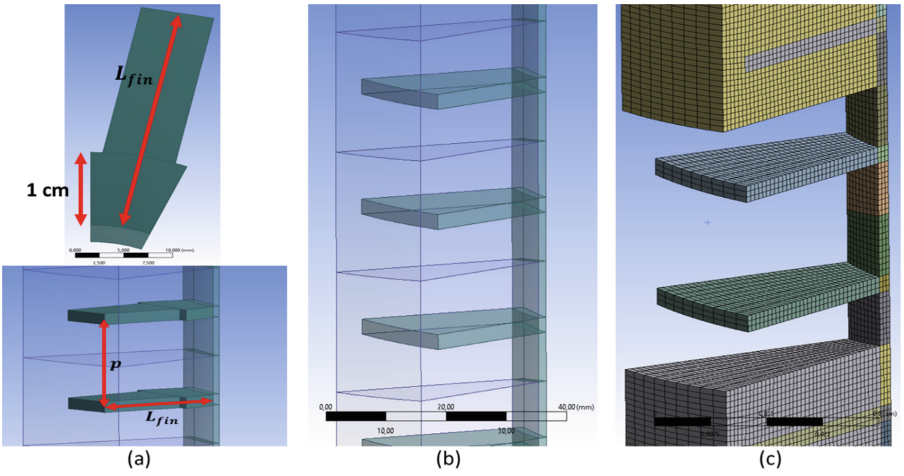

Fig. 1. Description of the geometries and mesh (a) serrated fins (b) circular fins (c) mesh

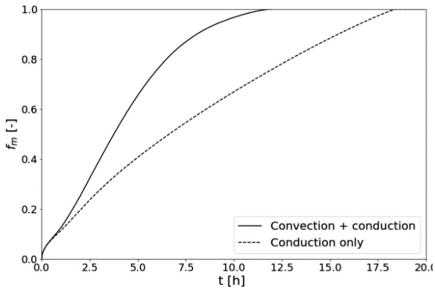

Fig. 2. Evolution of the melted fraction for a vertical smooth-tube TES with respect to time

Adiabatic and symmetry conditions are imposed on the outer and lateral boundaries respectively.

Hexahedron elements are adopted to discretize the finned tube and PCM domains (Fig. 1 (c)). The Computational Fluid Dynamics (CFD) simulations are performed with ANSYS Fluent software. PISO scheme is adopted for the pressure-velocity coupling; a second-order upwind scheme is used for the convective terms in the momentum and energy equations and a least-square cell-based scheme for the diffusive terms. PRESTO! scheme is used for spatial discretization of pressure equation. The under-relaxation factors for the pressure correction, momentum, energy and liquid fraction update are set as 0.9, 0.7, 1 and 0.9 respectively. A fixed time step of 0.05 s is adopted in the model where natural convection is considered, while a time step of 2 s is considered for the "conduction-only" model. A relative decrease value of 10^3 for the continuity and momentum equations is considered as convergence condition. For the energy equation, the residuals are kept below 10^{-11}.

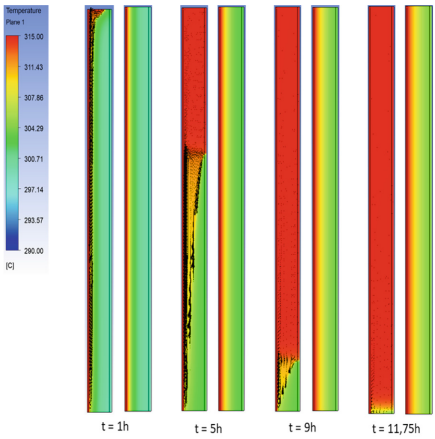

Fig. 3. Temperature and velocity contours in a vertical plane for a smooth-tube TES at different instants for two numerical models: left (convection + conduction), right (conduction-only)

3 Results and Discussions

3.1 Effect of Natural Convection on the Melting Process in Vertical Smooth-Tube TES

During the charge phase, PCM undergoes a solid-liquid phase transition that generates, with the increase of the melted fraction, vertical movements in the liquid phase due to the buoyancy difference. Therefore, local natural convection, occurring in the liquid PCM, may enhance significantly the heat transfer and the evolution of the melted front. In order to quantify its effects on the thermal power of the storage, the results obtained from the two heat transfer and phase change models described in the previous section will be presented. Before studying the impacts caused by the addition of different fins' configurations, simulations were carried on a vertical smooth-tube TES with no fins. This configuration will be later used as a reference to estimate the improvements of the storage's thermal power due to integration of different fins' configurations.

Figure 2 presents the evolution of the melted fraction defined by Eq. (5) during the charge. The resulting curves from the two numerical models overlap for a melted fraction under 10%. At this stage, most of the PCM is still in solid phase and therefore, natural convection has little to no effects on the total thermal power of the system. Through time, the PCM melted fraction increases and natural convection enhances the melting process. At any given moment, the melted fraction predicted by the convection + conduction model is significantly higher than that predicted by the conduction-only model. As a result, by considering local natural convection, the PCM's total melting time dropped from 18.4 h to 11.9 h, a reduction factor of 1.54. This result highlights, at a global scale, the importance of considering fluid circulations in liquid phase.

Figure 3 shows temperature and velocity fields in the PCM region at different instants during the charge phase. For each instant, a contour obtained from the conduction-only model (on the right) is compared to the one obtained from the convection + conduction model (on the left). Since a uniform temperature of 315 °C is imposed at the inner wall of the heat transfer tube, the results issued from the conduction-only model show a uniform melting front, with a uniform temperature distribution along the vertical direction progressing gradually between the tube's outer wall and the outer limit of the calculation domain. For the convection + conduction model, the circulations of the liquid PCM causes the deformation of the melting front. Therefore, more PCM is melted, with higher temperature values, at the top of the domain with respect to the bottom. At $t = 5$ h for example, the melting front has already reached the outer boundary of the domain in a region at the top where the PCM's temperature reaches the threshold value of 315 °C. The vertical length of this region increases with the progress of the charge phase resulting in an almost full melted PCM at $t = 11.75$ h compared to a melted fraction of 75% for the conduction-only model after the same charging time.

The results discussed in this section demonstrated the important impact that natural convection has on the melting process at local and global scales. For that reason, a similar comparison will be considered to quantify the effects of convection when radial metallic fins are added to the system.

3.2 Effect of Fin Number

In this section, the effects of the fin number on the overall thermal performance of a LHTES during the charge phase will be investigated. Generally, highly conductive metallic fins are added to the external surface of the heat transfer tubes to compensate for the low thermal conductivity of PCMs. However, for a given tube length, since natural convection in the liquid phase has a significant impact on the total melting time, one does not expect a linear relationship between the number of fins and the rate of improvement of the system's thermal power. To study the impact of fin number on the melting process for a given tube geometry, standard circular fins following a helical pattern (Fig. 1 (a)) are used. The configurations retained in this section are the following: N = 18, 27, 40, 54 and 80 with a fin length L_{fin} of 26 mm and fin thickness e_{fin} of 2.5 mm. For each configuration, two simulations are performed, a first one using the conduction-only model and a second one considering natural convection.

Figure 4 compares the temperature and velocity contours in the PCM region obtained from the conduction-only and convection + conduction models at three different instants during the charge phase. At t = 0.25 h, the PCM is already around the solidus temperature of 303.3 °C in all configurations. The effect of fin number on the melting's progress is already visible at this stage. However, the results obtained from both numerical models are in good agreement. This is no more the case for t = 1 h, when the volume of the liquid phase becomes relatively important to engender natural convection and result in a non-uniform melting front where more PCM is melted at the top of the domain. The melting front has already reached the external boundary in the configurations with high fin number.

On the contrary, it is still confined between the fins in the configuration with the lowest fin number (N = 18). Since a uniform temperature is considered as a boundary condition on the internal tube's surface, the conduction-only model results in a uniform temperature distribution in the axial direction. At t = 1.75 h, the temperature has already achieved its maximum value of 315 °C in the configurations with high fin number signalling the end of the charge process. Furthermore, the temperature distribution difference between the two models increases when the space between two fins in the axial direction increases.

To quantify the effects of fin number and of natural convection on the melting process, Fig. 5 shows the evolution of the melted fraction f_m with time resulting from the two models for each configuration. It shows that f_m increases when N is more important. The total melting time using the convection + conduction model with an increasing order of N is respectively 2.44, 1.89, 1.56, 1.46 and 1.33 h.

Compared to a melting time of 11.9 h for a smooth-tube TES, the addition of any number of fins leads to a significant reduction in the total melting time. Furthermore, the rate of improvement due to fin addition decreases with the increase of N. For example, the total melting time decreases by 22.5% by adding 9 fins (cases with N = 18 and 27) but it only decreases by 14.7% when adding 40 more fins and doubling the fin number from 40 to 80. This can be seen in Fig. 5 where the difference in the values of f_m obtained from the conduction-only and convection + conduction models is largely dependent of N. This gap decreases with the addition of more fins. Moreover, it depends on the state of the PCM. For example, in the case with 80 fins, the two curves overlap until f_m reaches a value around 60%. Thus, the rate of variation of f_m varies according the storage's state.

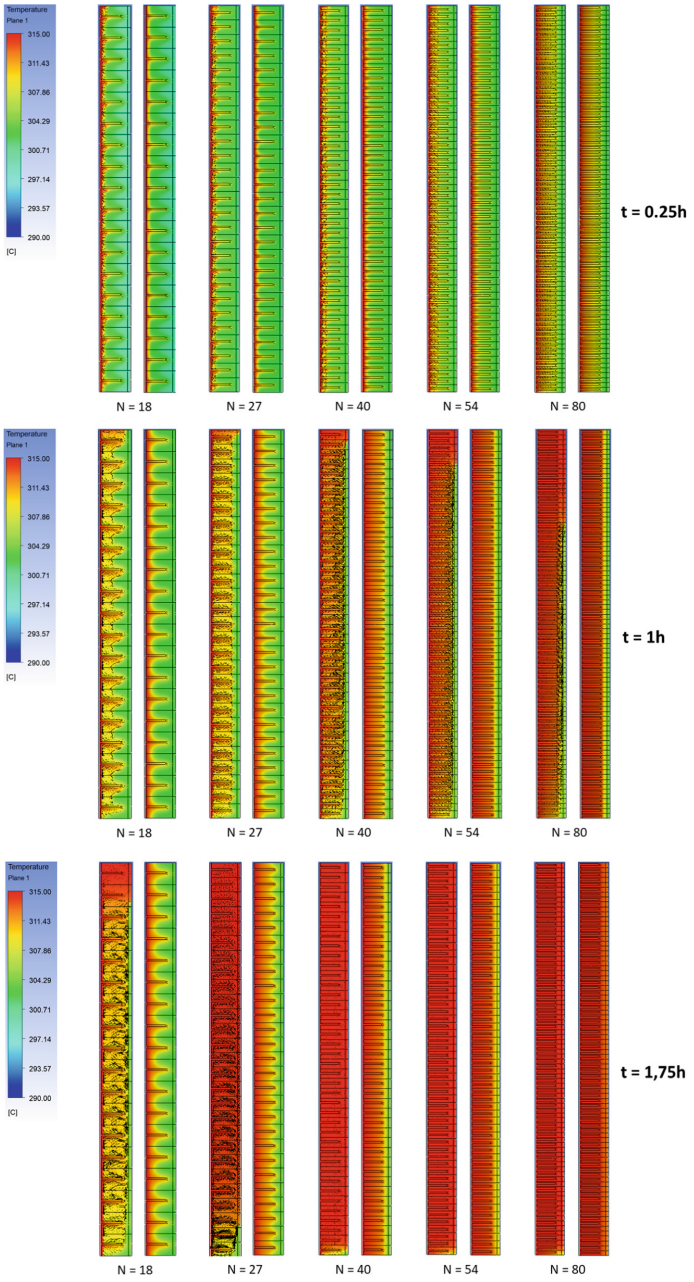

Fig. 4. Temperature and velocity contours in a vertical plane passing through the centre of the fins for different fin number at different instants: left (convection + conduction), right (conduction-only)

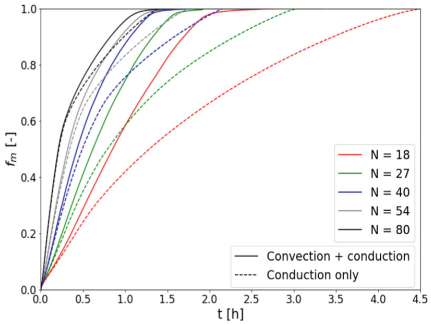

Fig. 5. Evolution of the melted fraction with time for different fin number

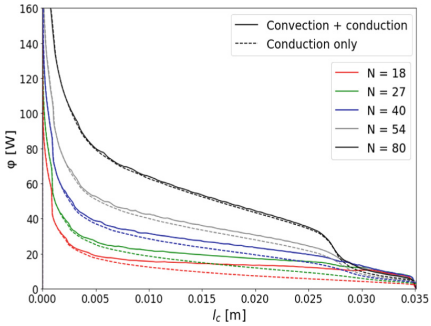

Fig. 6. Evolution of the total heat flux with respect to the thickness of the liquid phase for different fin number

To investigate this dependency, Fig. 6 shows the evolution of the total heat flux exchanged on the tube's inner wall surface with respect to l_c which is a characteristic length that represents an average position of the melting front separating both liquid and solid phases of PCM. To estimate the values of l_c from the melted fraction f_m, we consider that the liquid phase occupies an annular volume around the heat transfer tube truncated by the presence of the fins. For circular shaped fins, l_c is obtained by Eq. (7).

For a small volume of liquid PCM, with $l_c < 0.003$ m, even though the total heat flux is proportional to the fin number N, both heat transfer models predict the same values, natural convection has no significant role at this stage. With the progress of PCM's melting, the effect of natural convection in the liquid phase becomes notable for the configurations with relatively smaller fin number. For the configurations with higher fin number, the heat flux decreases progressively with the evolution of the melting front, until reaching a critical value of l_c around 0.026 m where the curves drops significantly and the heat flux predicted by the convection + conduction model became independent on the fin number. These results demonstrate that, once the melting front passes the tip of fins, the impact of fin addition on the storage's thermal power becomes negligible.

3.3 Effect of Fin Length

In the previous section, results showed that the total heat flux exchanged with the storage material is affected by the position of the melting front. Subsequently, the impact caused by the presence of fins on the total heat flux vanishes when the melting front exceed the tip of the fin. Building on that, the influence of fin length on the melting process of a LHTES will be investigated in this section. The configurations studied consist of 27 circular radial fins following a helical pattern, with a thickness $e_{fin} = 2.5$ mm. Four different fin length are presented, $L_{fin} = 22$, 26, 30 and 34 mm. As for the previous sections, the effects of natural convection on the melting process are investigated by performing two simulations for each configuration using the heat transfer models described earlier.

In Fig. 7, the evolution of the melted fraction f_m with time is plotted for each configuration. Intuitively, the longer the fin is, the faster the melting process is. From the convection + conduction model, the total melting times for different configurations with a fin length increasing from 22 to 34 mm are respectively 2.66, 1.89, 1.4 and 1.24 h. If we compare these results with the corresponding total melting time obtained from the conduction-only model of 4.17, 2.98, 2.15 and 1.98 h, we find an improvement ratio on the PCM's total melting due to natural convection in the liquid phase of 36, 36.7, 35 and 37.2% respectively according to an increasing in the length of the fin. We can deduce that, although natural convection still has a significant impact on the melting process, this impact does not depend directly at global scale on the fins' length.

As in the previous section, Fig. 8 shows the evolution of the total heat flux with respect l_c, which is defined – since circular fins are used in this study – by Eq. (7). For a melting front position close to the tube's external surface (relatively small l_c), the heat flux exchanged in the storage is independent of the fin's length and of the heat transfer mechanism within the PCM. Then, with the melting front progression, the gap between the results obtained from the two different heat transfer models increase, this is due to the liquid PCM circulations in the sub volumes between two radial fins in the axial direction, which enhance convective heat transfers. Approaching the fin's tip, the PCM's temperature rises, which increases the thermal resistance of the system and therefore, the total heat flux drops.

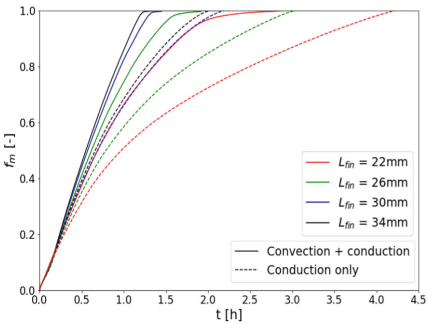

Fig. 7. Evolution of the melted fraction with time for different values of the fin length

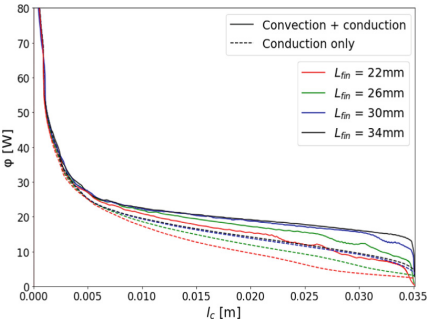

Fig. 8. Evolution of the total heat flux with respect to the thickness of the liquid phase for different values of the fin length

$$l_c = \begin{cases} -R_{t,ext} + \sqrt{R_{t,ext}^2 + \frac{V_{MCP,tot}}{\pi p\left(1-\frac{e}{p}\right)} f_m} & for\, f_m < \frac{\pi p\left(1-\frac{e}{p}\right)\left(\left(R_{t,ext}+L_{fin}\right)^2 - R_{t,ext}^2\right)}{V_{MCP,tot}} \\ -R_{t,ext} + \sqrt{\frac{V_{MCP,tot} f_m - \pi p\left(1-\frac{e}{p}\right)\left(\left(R_{t,ext}+L_{fin}\right)^2 - R_{t,ext}^2\right)}{\pi p} + \left(R_{t,ext}+L_{fin}\right)^2} & for\, f_m > \frac{\pi p\left(1-\frac{e}{p}\right)\left(\left(R_{t,ext}+L_{fin}\right)^2 - R_{t,ext}^2\right)}{V_{MCP,tot}} \end{cases} \tag{7}$$

To study the impact of natural convection at a local scale along the tube on the melting process, Fig. 9 illustrates the temperature and velocity contours at three instants for the configurations with different fin length obtained from the two heat transfer models (conduction-only and convection + conduction). At t = 0.25 h, PCM is near the solidus temperature, both models predict similar temperature distribution. The effects caused by the fin's length is inconsiderable at this stage. At t = 1 h, in the configurations with relatively shorter fins, the melting front separating the solid phase from the liquid phase is continuous along the axial direction and has already exceeded the tip of the fins. For the longest fins (L_{fin} = 34 mm), the heat transferred to the PCM via the fins' surface at its tip divides the solid PCM into sub-volumes confined between the radial fins. Another important observation from these contours is that, the use of long fins extended to the external frontier of the domain results in an almost uniform melting front along the vertical direction. For shorter fins, when the melted front exceed the fins' tip (at t = 1.75 h), the heat flux exchanged within the liquid phase in the upward direction has a significant impact on the temperature distributions in the storage.

3.4 Effect of Fin Type

Now, the effect of the fin type of the melting process will be investigated. For that purpose, circular and serrated radial fins following both a helical pattern and having the same thermal properties are used (Fig. 1). For both types, the configuration with 27 fins of length L_{fin} = 30 mm and thickness e_{fin} = 2.5 mm is retained.

Figure 10 illustrates the temperature and velocity contours in a vertical plane passing through the centre of the fins. For both types, natural convection plays no big role at t =

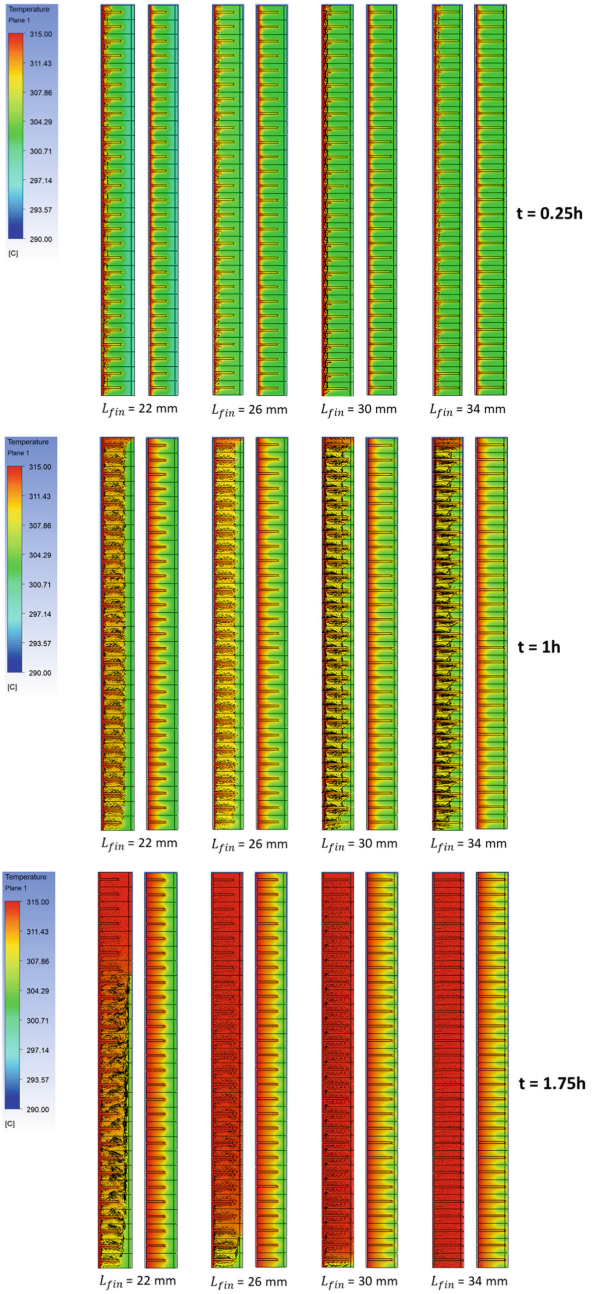

Fig. 9. Temperature and velocity contours in a vertical plane passing through the centre of the fins for different fin length at different instants: left (convection + conduction), right (conduction-only)

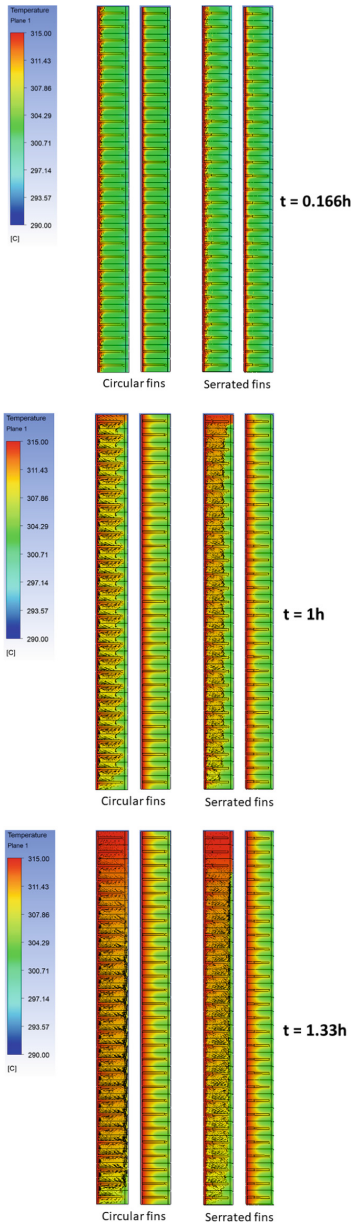

Fig. 10. Temperature and velocity contours in a vertical plane passing through the centre of the fins for two fin types at different instants: left (convection + conduction), right (conduction-only)

0.166 h. Both heat transfer models predict a uniform temperature distribution in the axial direction. The differences appear at t = 1 h, where, the temperature distribution predicted by the convection + conduction model is slightly advanced with respect to the uniform

one predicted by the conduction model. Furthermore, from the temperature contours at this instant, we can qualitatively observe that the average temperature of liquid PCM (region where the temperature is above the liquidus temperature of 306.6 °C) is more important for serrated fins. This is because the geometric form of serrated fins promotes vertical circulations of the liquid phase between the rectangular branches of two fins in the angular direction, which enhance natural convection. At t = 1.33 h, the temperature distribution difference obtained from both models is more remarkable. The charge is almost finished for circular fins using the convection + conduction model. Compared to serrated fins, circular fins having the same fins' configuration result in a faster melting process.

Figure 11 shows the evolution of the melted fraction f_m with time. As seen before, at the initial stage of the melting process, the effects of natural convection are negligible for both fins. Additionally, at this stage, the geometric type of the fin has no significant impact on the system's thermal power. The additional surface area for circular fins does not contribute to the total heat flux. With the progress of the melting front, the use of circular fins enhances the total heat exchanged to the storage resulting in a faster PCM melting and a higher thermal power. The total melting time for circular fins is 1.4 h compared to 2.06 h for serrated fins. Generally, the interest of using serrated fins is to benefit from natural convection enhancements due to liquid PCM circulations in the annular space between two rectangular branches of the fins. To validate this, Fig. 12 shows the variation of the time ratio to melt a PCM fraction f_m prediction by both numerical models: conduction-only and convection + conduction. The time ratio $t_{c/cc}$ is calculated as follow:

$$t_{c/cc} = \frac{t_{conductiononly}}{t_{conduction+convection}}. \tag{8}$$

The graph shows that the value of $t_{c/cc}$ increases with the melted fraction f_m for both fin types, which means that the effects of natural convection are more important evident when the liquid phases' volume increases. However, this ratio is more important for serrated fins type. As we can see in Fig. 11, the activation of natural convection thighs the gap between the curves obtained for the two fin types. At the end, even though natural convection plays a more important role in serrated fins, the system's overall thermal

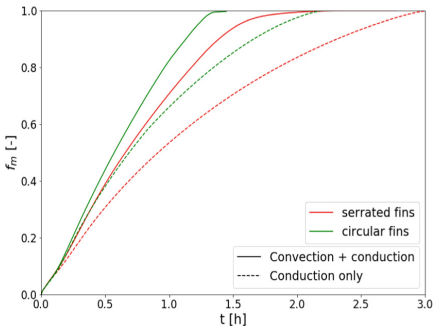

Fig. 11. Evolution of the melted fraction with time for two fin types

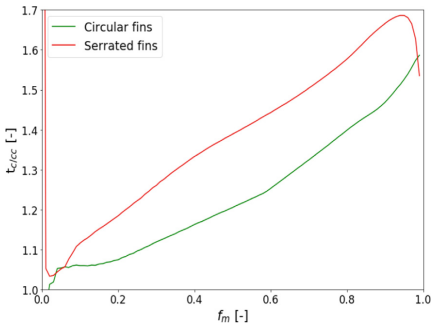

Fig. 12. Evolution of the time ratio from both heat transfer models as function of the PCM's melted fraction.

power is affected in the first order by the fins' surface. A more pertinent conclusion could be drawn by comparing the outcome from all the studied configurations when applied to a storage sizing with given design parameters.

3.5 Application to Storage Sizing

In the previous sections, investigations were made to quantify the effects of fins' geometry and natural convection enhancements on the storage performances during charge phase. However, since the design parameters of the computational domain, defined by the tube's length and external diameter were identical for all the configurations, this leaves us with a variable volume fraction of PCM with respect to the total volume of the system. In other words, the mass of the PCM is not the same in all configurations, which means that the energy stored during charge phase is not identical. Therefore, an alternative way to compare the outcome from different configurations for the two studied fin types based on the convection + conduction model is presented in this section. The idea is to fix two important design parameters, which are the amount of energy stored in the system and time taken to store that energy. Then, a set of fins configurations that permit to reach these criteria is obtained.

Figure 13 shows the time taken by the system to store 0.65 kWh/ m of tube for each fins' configuration. On the x-axis, the heat transfer surface is the area defined by the external tube and fins in contact with the PCM for a tube length of 1 m. For an optimal design, the objective is to decrease the volumetric fraction of metallic fins and reduce as much as possible the heat transfer surface. The horizontal dashed lines represent the time target set as a design parameter. In this case, we consider two arbitrary examples. In the first one, we consider charging the 0.65 kWh in less than 1.5 h. While in the second one, a threshold time of 1.1 h is considered to charge the very same energy. Results demonstrate that the time needed to reach the desired stored energy is usually longer for serrated fins. Moreover, for this fin type, the configurations with a fin number of 18, 27 and 54 show that the elongation of the fins over 30 mm does not lead to a significant improvement to time parameter. If we now compare the curves obtained from the configurations with different fin number, we observe that the time taken to store the 0.65 kWh decreases asymptotically with the increase of the fin number. Therefore, as for the fins' length, the

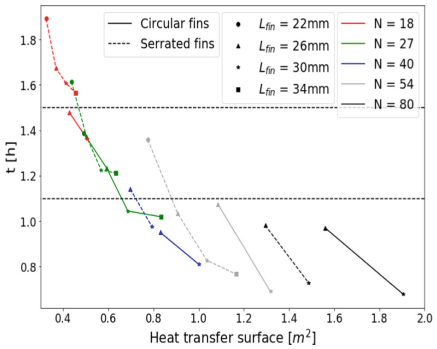

Fig. 13. Evolution of the time taken to charge 0.65 kWh/ m tube as function of the heat transfer surface for the studied configurations

rate of improvement due to fin addition will decrease. From the results, we can find that, except for the configurations with N = 18 and (N = 27, L_{fin} = 22 mm) serrated fins, all the others permit to store the energy while respecting the time threshold of 1.5 h. The list of suitable configurations is narrowed down in the case with a lower time threshold of 1.1 h, where, a higher thermal power is required by the system to respond to the design criteria. As a results, in this case, the optimal configuration with the lowest fin number possible, resulting in a relatively low heat transfer surface while respecting the imposed parameters of 0.65 kWh/ m and a charging time of 1.1 h would be the one with 27 circular fins of length L_{fin} = 30 mm and thickness e_{fin} = 2.5 mm.

4 Conclusion

This study demonstrated the effect of adding radial fins on the thermal performances of a shell-and-tube LHTES for a given tube length. The investigations of the impact of different parameters can be resumed as follows:

- For a smooth-tube TES with a uniform temperature imposed as a boundary condition on the internal tube wall, natural convection affects significantly the melting process at both, global and local scales. The PCM's total melting time was reduced by a factor of 1.54 times when natural convection was considered in the liquid phase.
- Compared to a smooth-tube TES, the addition of 18 fins (equivalent of 33 fin/m) reduces the total melting time to the fifth. Further increase of the fin number resulted in a uniform melted front and a lower total melting time. However, it was shown that due to the restriction of natural convection in the space between two fins, the rate of improvement due to fin addition decreases with the increase of the fin number.
- Even though the shape of the melting front and the total melting time are affected by the fins' length, the improvement ratio of the total melting time due to the consideration of natural convection is independent of the fins' length.

- The comparison between two radial fin types demonstrated that the use of serrated fins enhances natural convection. However, for the same fins' configuration, circular fins result in a faster melting.

In addition to the fins' number, length and type. Another design parameter that can influence the storage's thermal power and natural convection is the fins' thickness. Complementary cases will be simulated considering the variation of this parameter will allow the comparison of different configurations having an identical PCM's volume. Moreover, the results obtained from these studies will be used to find dimensionless correlations on the system's thermal power according to the fins' geometric configurations.

References

1. D. Laing, T. Bauer, N. Breidenbach, B. Hachmann, et M. Johnson, «Development of high temperature phase-change-material storages», *Appl. Energy*, vol. 109, p. 497-504, sept. 2013, doi: https://doi.org/10.1016/j.apenergy.2012.11.063.
2. M. Johnson, J. Vogel, M. Hempel, A. Dengel, M. Seitz, et B. Hachmann, « High Temperature Latent Heat Thermal Energy Storage Integration in a Co-gen Plant », *Energy Procedia*, vol. 73, p. 281-288, 2015, doi: https://doi.org/10.1016/j.egypro.2015.07.689.
3. I. E. Agency, *Energy and climate change: world energy outlook special report*. International Energy Agency, 2015.
4. M. Jiménez-Arreola, R. Pili, F. Dal Magro, C. Wieland, S. Rajoo, et A. Romagnoli, « Thermal power fluctuations in waste heat to power systems: An overview on the challenges and current solutions », *Appl. Therm. Eng.*, vol. 134, p. 576-584, avr. 2018, doi: https://doi.org/10.1016/j.applthermaleng.2018.02.033.
5. S. S. Mostafavi Tehrani, G. Diarce, et R. A. Taylor, « The error of neglecting natural convection in high temperature vertical shell-and-tube latent heat thermal energy storage systems », *Sol. Energy*, vol. 174, p. 489-501, nov. 2018, doi: https://doi.org/10.1016/j.solener.2018.09.048.
6. S. Zhang, L. Pu, L. Xu, et M. Dai, « Study on dominant heat transfer mechanism in vertical smooth/finned-tube thermal energy storage during charging process », *Appl. Therm. Eng.*, vol. 204, p. 117935, mars 2022, doi: https://doi.org/10.1016/j.applthermaleng.2021.117935.
7. F. Agyenim, P. Eames, et M. Smyth, « A comparison of heat transfer enhancement in a medium temperature thermal energy storage heat exchanger using fins », *Sol. Energy*, vol. 83, n° 9, p. 1509-1520, sept. 2009, doi: https://doi.org/10.1016/j.solener.2009.04.007.
8. A. Rozenfeld, Y. Kozak, T. Rozenfeld, et G. Ziskind, « Experimental demonstration, modeling and analysis of a novel latent-heat thermal energy storage unit with a helical fin », *Int. J. Heat Mass Transf.*, vol. 110, p. 692-709, juill. 2017, doi: https://doi.org/10.1016/j.ijheatmasstransfer.2017.03.020.
9. R. Karami et B. Kamkari, « Experimental investigation of the effect of perforated fins on thermal performance enhancement of vertical shell and tube latent heat energy storage systems », *Energy Convers. Manag.*, vol. 210, p. 112679, avr. 2020, doi: https://doi.org/10.1016/j.enconman.2020.112679.
10. X. Yang, Z. Lu, Q. Bai, Q. Zhang, L. Jin, et J. Yan, « Thermal performance of a shell-and-tube latent heat thermal energy storage unit: Role of annular fins », *Appl. Energy*, vol. 202, p. 558-570, sept. 2017, doi: https://doi.org/10.1016/j.apenergy.2017.05.007.
11. Z.-G. Shen, S. Chen, et B. Chen, « Heat transfer performance of a finned shell-and-tube latent heat thermal energy storage unit in the presence of thermal radiation », *J. Energy Storage*, vol. 45, p. 103724, janv. 2022, doi: https://doi.org/10.1016/j.est.2021.103724.

12. X. Yang, X. Wang, Z. Liu, X. Luo, et J. Yan, « Effect of fin number on the melting phase change in a horizontal finned shell-and-tube thermal energy storage unit », *Sol. Energy Mater. Sol. Cells*, vol. 236, p. 111527, mars 2022, doi: https://doi.org/10.1016/j.solmat.2021.111527.
13. A. Shahsavar, A. Goodarzi, H. I. Mohammed, A. Shirneshan, et P. Talebizadehsardari, « Thermal performance evaluation of non-uniform fin array in a finned double-pipe latent heat storage system », *Energy*, vol. 193, p. 116800, févr. 2020, doi: https://doi.org/10.1016/j.energy.2019.116800.
14. A. Lomonaco, D. Haillot, E. Pernot, E. Franquet, et J.-P. Bédécarrats, « Sodium nitrate thermal behavior in latent heat thermal energy storage: A study of the impact of sodium nitrite on melting temperature and enthalpy », *Sol. Energy Mater. Sol. Cells*, vol. 149, p. 81-87, mai 2016, doi: https://doi.org/10.1016/j.solmat.2015.12.043.
15. V. R. Voller et C. Prakash, « A fixed grid numerical modelling methodology for convection-diffusion mushy region phase-change problems », *Int. J. Heat Mass Transf.*, vol. 30, n° 8, Art. n° 8, août 1987, doi: https://doi.org/10.1016/0017-9310(87)90317-6.
16. C. Beust, E. Franquet, J.-P. Bédécarrats, et P. Garcia, « A numerical investigation of some key factors for the simulation of convection-dominated melting », *Int. J. Therm. Sci.*, vol. 161, p. 106687, mars 2021, doi: https://doi.org/10.1016/j.ijthermalsci.2020.106687.
17. C. Beust, E. Franquet, J.-P. Bédécarrats, et P. Garcia, « Predictive approach of heat transfer for the modelling of large-scale latent heat storages », *Renew. Energy*, vol. 157, p. 502-514, sept. 2020, doi: https://doi.org/10.1016/j.renene.2020.04.135.